June, 1989

NiFe INVAR Alloys: Theoretical Insights into the Underlying Mechanisms Responsible for Their Physical Properties

Duane D. Johnson, *Sandia National Laboratories*
F. J. Pinski, *University of Cincinnati*
J. B. Staunton, *University of Warwick*
B. L. Gyorffy, *University of Bristol*
G. M. Stocks, *Oak Ridge National Laboratory*

SANDIA REPORT

SAND89-8504
Unlimited Release
Printed June 1989

NiFe INVAR Alloys: Theoretical Insights into the Underlying Mechanisms Responsible for Their Physical Properties

(To be published in Physical Properties of Low-Expansion (INVAR-type) Alloys, ed. Ken Russell, Materials Research Society, 1989)

D. D. Johnson, F. J. Pinski, J. B. Staunton, B. L. Györffy, G. M. Stocks

Prepared by
Sandia National Laboratories
Albuquerque, New Mexico 87185 and Livermore, California 94551-0969
for the United States Department of Energy
under Contract DE-AC04-76DP00789

Issued by Sandia National Laboratories, operated for the United States Department of Energy by Sandia Corporation.

SAND89-8504
Unlimited Release
Printed June 1989

NiFe INVAR ALLOYS: THEORETICAL INSIGHTS INTO THE UNDERLYING MECHANISMS REPONSIBLE FOR THEIR PHYSICAL PROPERTIES.

D. D. Johnson[1], F. J. Pinski[2], J. B. Staunton[3], B. L. Györffy[4], and G. M. Stocks[5]

[1]Sandia National Laboratories, Livermore, CA 94551-0969

[2]University of Cincinnati, Cincinnati, OH 45220

[3]University of Warwick, Coventry, U. K. CV4 7AL

[4]University of Bristol, Bristol, U. K. BS8 1TL

[5]Oak Ridge National Laboratory, Oak Ridge,TN 37831

ABSTRACT

What are the "driving forces" responsible for various physical properties of alloys? What causes alloy systems to order chemically and/or magnetically? To answer these questions, we have been using a quantum mechanical (QM) method to calculate cohesive energies, magnetic properties, and thermodynamic phase instability of alloys. This scheme directly incorporates the inherent disorder of the high-temperature solid solution and in this sense goes beyond traditional "band theory." Although approximations have been made at various steps in the thermodynamical averaging, and in the QM treatment of the electrons, adjustable parameters have not been used. Recently, for FCC NiFe (INVAR) alloys, we have calculated cohesive energies and magnetizations for several concentrations, including Ni-35%, and, also, the short-range ordering instabilities in the Ni-rich alloys to investigate the strong interplay between magnetism and concentration fluctuations. We describe the current picture of NiFe INVAR alloys that emerges from our calculations.

1. INTRODUCTION

When the states of magnetic and compositional order are strongly coupled in alloys, a number of physically interesting and technologically important phenomena arise. For example, when cooled in a magnetic field from high temperatures, nickel-rich Ni_cFe_{1-c} alloys chemically order preferentially along the magnetic field direction (1). Also, some alloys, such as $Ni_{0.35}Fe_{0.65}$, at room temperatures do not expand or contract with changes in temperature. This is the so-called INVAR (volume INVARiance) effect, in which magnetism plays the all important role, as we shall see. In the early part of this century, this property of NiFe allowed the Swiss watch industry to prosper because their watches could keep proper time, independent of the temperature. This property of the alloy was deemed so important that a Nobel Prize was awarded to its discoverer, Guillaume. Even today the properties of INVAR alloys are technologically important; for example, these alloys have applications as components in nuclear reactor walls to reduce temperature-cycle fatigue, in gas turbine engines and in calibration equipment for temperature stability. It is interesting that even after 80 years the INVAR alloys are still not fully understood! Naturally then, the study of how compositional and magnetic fluctuations influence one another has been pursued vigorously for many years (2). However, progress has been hampered for the most part because it is difficult to construct a theory which incorporates both kinds of fluctuations on an equal basis and in quantitative detail. In this paper, as an illustration of a step towards such a theory, we investigate the effects of magnetic order on the tendency towards compositional order and the effects of compositional changes on the state of magnetism in the Ni_cFe_{1-c} INVAR alloys within a fully parameter-free, electronic framework.

That the study suggested above might be a fruitful enterprise follows from fairly simple considerations. When Fe is added to Ni, at high temperatures where they form a FCC solid solution, both the Curie temperature, T_C, and the average moment, $\bar{\mu}$, per site rises with increasing iron concentration. Suprisingly, near $c \approx 0.75$, T_C begins to decline while $\bar{\mu}$ continues to increase until reaching the INVAR region ($c \approx 0.36$) where $\bar{\mu}$ collapses. A plausible explanation for this unexpected behavior is that the magnetic interaction between local moments on the Fe sites is antiferromagnetic (AFM) and this destabilizes the ferromagnetic (FM) state once the number of nearest-neighbor Fe pairs is large enough. Simple, spin-only models based on this idea do reproduce the above experimental observations (3). [Roughly speaking, T_C is proportional to the effective interactions between moments; thus, although the moments in a system may be increasing, their effective interactions and T_C may increase (as it does in a FM) or decrease (as it can in an AFM).] Moreover, there is first-principles theoretical evidence that Fe on an FCC lattice, with a lattice parameter close to that of the Ni_3Fe alloy, would be antiferromagnetic (4). Such antiferromagnetic frustration is also predicted by Kakehashi (5) and Hasagawa (6) on the basis of simple, itinerant models. As we shall see, this is only part of the mystery, and, as is the case in good mysteries, there is always a twist. Nonetheless, taken at face value, the above physical picture implies a strong tendency towards chemical order in order to reduce the number of nearest-neighbor Fe pairs. Indeed, Ni_cFe_{1-c} orders into the $L1_2$ structure at $c \approx 0.75$ and into the $L1_0$ structure at $c \approx 0.50$.

In general, theoretical understanding of the physical properties of most technologically important alloys has evolved from an investigation of ordered elements and compounds. Yet, it is worth noting that most of these alloys, whether magnetic or not, exhibit some type of disorder, especially above room temperature. We have formulated a theory which addresses the most common form of disorder in metallic alloys, that of substitutional randomness. In contrast to amorphous alloys, random substitutional alloys (RSA) possess an underlying lattice of well-defined atomic positions; however, these lattice sites are occupied randomly by the various constituents, constrained only by the chemical composition of the alloy. We have reviewed this theory (7) and the progress that we have made in investigating the effects of disorder in alloys, the associated equilibrium properties, and possible ordering instabilities (short-range order) in non-magnetic alloys, etc. Moreover, we emphasized that the overall goal is to make progress with the more general problem of predicting the relative stability of different alloy phases and to design specialty alloys from computations as an economically feasible alternative to long hours in the laboratory . In this paper, a generalization of this theory which incorporates magnetism (8) is applied to Ni_cFe_{1-c} INVAR alloys. Our principle aim is to use reliable and parameter-free calculations to investigate the plausibility of the suggestion that the chemical order in these alloys is of magnetic origin and that the underlying

magnetic interactions change with Fe additions. Indeed, the current picture which emerges from our calculation suggests that magnetism plays the dominate role in a majority of the physical properties of INVAR alloys.

As a point of information, the development of this theory of magnetic, disordered alloys and their chemical ordering instabilities was only possible with a concurrent advance in the power of supercomputers. For example, in some of the calculations described in this paper, we have used hundreds of hours on a CRAY-XMP!! Still, if not for concomitant advances in both the algorithms and the theory with the power of the supercomputers, we would have required 10-100 times that amount. As it is not the purpose of this paper to review the theory and methods necessary to solve the magnetic, random substitutional alloy problem, we refer the reader to Ref. 7, and references therein, for more details.

This paper is organized into five sections. In the next section, we present an overview of the parameter-free approach developed to describe accurately disordered alloys and their energetics. As many review articles exist (9), this section will be only descriptive. In Section Three, we develop some simple ideas of how magnetism can influence electronic states in alloys, as well as some simple terminology that will aid in later discussion. Section Four is a concise presentation of a response theory for the static, high-temperature susceptibility. Namely, in Section 4a. we discuss the so-called "disordered local moments" (DLM) state which theoretically represents the state of magnetic disorder (i.e., magnetic fluctuations) in systems above T_C. Investigation of the DLM state allows study of the magnetic correlations and transition temperature. In Section 4b., we investigate the short-range order instability (i.e., chemical fluctuations) in $Ni_{0.75}Fe_{0.25}$ and its origin. We also calculate the effect of chemical environment changes on the magnetic properties, such as occurs upon ordering. In Section 4c., we describe our results for the $Ni_{0.35}Fe_{0.65}$ alloy and discuss the importance of both magnetic and chemical fluctuations in giving rise to the anomalous properties of INVAR alloys. The concentration dependence of various properties are discussed in Section 4d. Finally, we present some conclusions in the summary.

2. ELECTRONS, DISORDER, AND ALLOYS

2a. OVERVIEW

When several physical effects are present, it is often misleading or difficult to interpret experimental data in terms of simple models. (This has clearly been the case for INVAR-type alloys.) Parameter-free approaches offer the hope of producing a theory with predictive powers and of unraveling the origins of various effects without relying on a predetermined bias. For metallic systems, the true many-electron problem (the electron "glue" which is responsible for cohesion in the metals) can be described fairly accurately by density-functional theory (DFT) (10). In essence, this allows the many-electron problem to be reduced to a single-electron problem in an *effective* potential field of the other electrons. In combination with DFT, the electronic structure of ordered metals may be found by any number of quantum mechanically based methods, such as the Green's function approach of Korringa, Kohn, and Rostoker (KKR) (11). For disordered alloys, the random location of constituent atoms produces a problem without translational symmetry which cannot be solved by traditional band-structure methods. The coherent-potential approximation (CPA) (12) is an effective medium approach for averaging the Green's function over the disorder. Because they both deal with the Green's function, the CPA and the KKR can be easily combined. The basic idea of the KKR-CPA method is that an array of randomly placed potentials can be replaced by an ordered array of energy dependent, effective potentials and the standard methods of calculating the electronic structure again may be used. The key then is to find the effective potential which best reproduces the configurationally averaged properties of the disordered alloy. Thus, for disordered alloys there are two different self-consistency procedures that are necessary, the charge self-consistency due to charge transfer, as in normal band-structure calculations, and the self-consistency procedure to determine the CPA effective medium. It is the determination of the CPA effective medium which is the crucial and time consuming step in disordered alloy calculations. Within the KKR-CPA approach these two self-consistency conditions are inextricably mixed together, but once completed, the lattice constants, heats of mixing, bulk

modulus, etc., may be determined and compared to experiment (13). In what follows, a brief description of self-consistent procedure in electronic structure calculations is given and how the CPA makes it possible to calculate properties of disordered alloys, such as total energies.

2b. THE SCF PROCEDURE

The self-consistent field (SCF) electronic structure calculations that are routinely performed today on ordered metals and compounds and disordered alloys all follow a similar procedure. The essential difference between the disordered and ordered calculation is the necessity of finding the effective scatterers via the CPA equations. For those unfamiliar with the structure of these types of calculations, the following flow chart, Fig. 1, represents the calculational procedure. $Z_{\alpha,i}$ and $\underline{R}_i$ refer to the atomic number of the constituent atoms and lattice site positions, respectively. "a" refers to the lattice constant, or distance between two successive lattice sites.

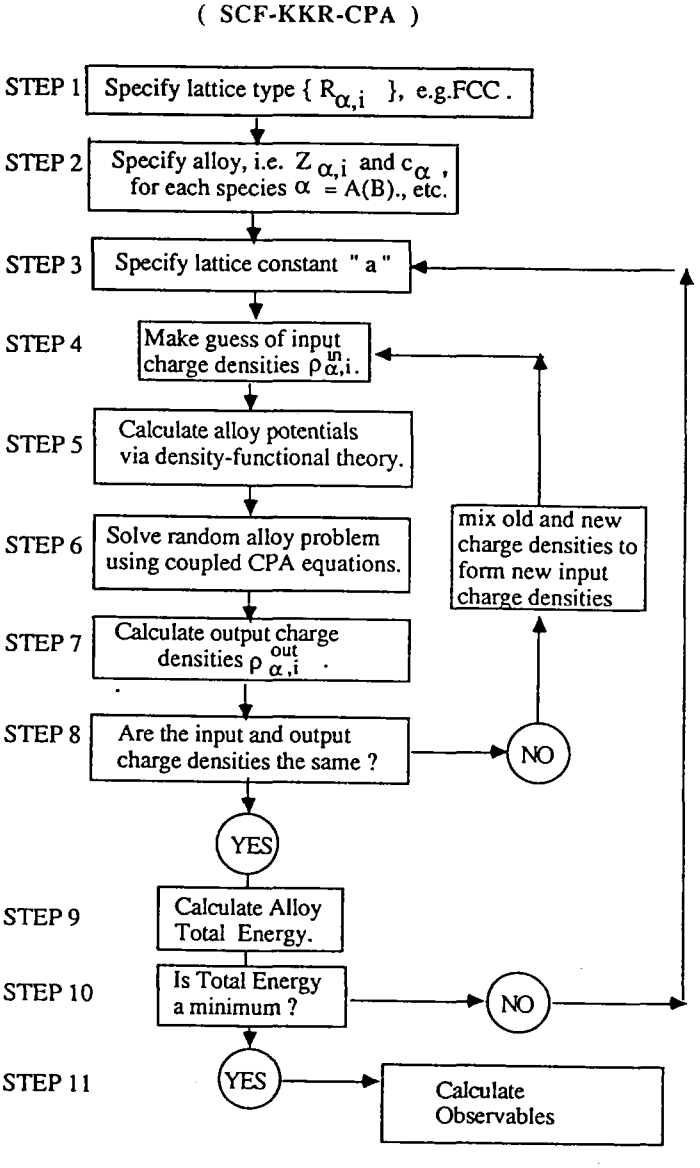

Fig. 1. A flow-chart of a typical self-consistency cycle for a KKR-CPA electronic structure calculation.

For a particular lattice symmetry, such as face-centered-cubic (FCC), and set of $\{Z_{\alpha,i}\}$, a choice of the lattice constant is made. From there the algorithm is followed until the charge densities converge. If the energy is not a minimum, another lattice constant is chosen and the algorithm is repeated. For a given alloy, this procedure is followed for each concentration of interest and for several different lattice constants. Both alloying properties and volume effects, for example, may be investigated. In Fig. 1, steps 5-9 in the self-consistency cycle are intimately connected and are the basis for all electronic structure calculations.

For a given occupation of lattice sites, a theorem **(10)** from density-functional theory states that the total energy functional of a collection of nuclei and electrons is a minimum only for the true ground state charge density, which is simply related to the Green's function. Knowing this functional determines the entire SCF procedure, because its variation with respect to charge density defines the effective potential, v(r), that the electron 'sees', which in turn determines the charge density and allows calculation of the energy functional! The SCF procedure seems well-defined, if the total energy functional is known. However, there is a problem if this is applied to the disordered alloys.

For an ordered AB alloy, there is only one way to arrange the atoms on the lattice in an ordered fashion, resulting in one energy; however, for the disordered AB alloy, there are an infinite number of possible lattice site occupations. To get the average energy of the system, the energies $E[V;\{\xi_i\}]$ for each alloy configuration $\{\xi_i\}$ need to be averaged over their associated probability $P[\{\xi_i\}]$. (Note, $\xi_i = 1$ or 0 if the site i is occupied by an A or B.) Thus, the configurationally averaged (T = 0 K) total energy is given as

$$\langle E \rangle = \bar{E} = \sum_{\{\xi_i\}} P[\{\xi_i\}]\, E[V;\{\xi_i\}] \quad . \qquad (1)$$

Clearly, one can not perform this average exactly. Without a definite expression for the average total energy, the alloy problem and self-consistency are intractable. This is where the CPA provides its great advantage. From the KKR-CPA it is possible to construct an approximate configurationally averaged total energy which has the proper variational form to reproduce the potential **(13)**. Thus, within KKR-CPA, the SCF procedure is intact for disordered alloys! We may now choose an alloy to investigate, fix the parameters in steps (1-3) in Fig. 1, and then begin the self-consistency procedure.

For use later, we note here that at finite temperatures the grand potential of the system is required. The grand potential is composed of the energy (in our case, from DFT), the entropy, and the various chemical potentials in the problem of interest; for instance, for the binary alloy problem, $\Omega = E - TS - \zeta N_{elec} - \nu N$, where T is the temperature, N_{elec} is the number of electrons, N is the total number of atoms in the system ($N = N_A + N_B$), ζ is the chemical potential of the electrons (the Fermi energy at T= 0 K), and ν is the chemical potential difference ($\nu_A - \nu_B$) of the atoms.

The above brief overview of local density functional theory in combination with the KKR-CPA method as applied to disordered alloys was intended to give some feel for first-principles, electronic structure calculations. This approach for both ordered and disordered alloys results in agreement, typically, of 1% (3-5%) for the lattice constant for non-magnetic (magnetic) alloys and 10-20% for the bulk moduli. The magnetic moments are usually in good agreement with experiment. (In our calculations we have not incorporated spin-orbit coupling and we use a gyromagnetic ratio of 2.) Technically, the discrepancies in these quantities as compared to experiment are due mainly to the local density approximations (LDA) for the important electronic exchange and correlation energies which are made in order to make DFT tractable. This is especially true in the case of magnetic calculations where the discrepancy between theory and experiment is greater.

3. THE UPS AND DOWNS OF MOMENT FORMATION AND BONDING

For an alloy, magnetism can have a profound influence on electronic states to produce a variety of phenomena. As a primer for what is to be discussed later about the NiFe systems, it is worthwhile to start from a simple-minded picture of alloying and the effect of magnetism, or

exchange-splitting. (Exchange-splitting arises from purely quantum mechanical effects due to the nature of the interactions between electrons.) Here we give two examples of the types of interesting phenomenon which can occur due to the interplay of alloying and magnetism. First, in BCC FeV alloys, the interplay of magnetism and alloying is described in which the spin-down electrons are seen to play a special role. And, second, we investigate NiFe alloys as an example of the special role spin-up electrons may play in determining the physical properties of these alloys. [In a solid, spin-up (-down) refers to whether the electron has its spin state aligned parallel (antiparallel) to the direction of magnetization. Thus, spin-up (-down) electrons are usually referred to as majority (minority) electrons, when speaking of ferro- or ferri-magnets, since there are more spin-up electrons than spin-down electrons which results in a net magnetization.]

A naive description of the energy levels of the Fe_cV_{1-c} system is shown in Fig. 2. Note, in a solid, the energy levels are broadened into energy bands due to the overlap of the electronic wavefunctions - the so-called band structure. Nevertheless, this picture gives a simple way of understanding some of the phenomena that can occur. The energy levels of the d-electrons of a pure Fe system are exchange split, i.e., it is energetically favorable to have a net magnetization. There is no exchange-splitting in pure vanadium, i.e. both spin-up and spin-down energy levels are equal, and the vanadium d-electron levels are much closer in energy to the spin-down d-electron levels of iron than they are to the spin-up levels. Thus, alloying V to Fe to obtain a BCC FeV alloy, as suggested in the r.h.s. of Fig. 2, interactions are introduced which have a larger effect on the minority spin levels (compared to the majority) since their energy separation is smaller. In other words, the Fe induces an exchange-splitting on the V sites in order to lower the kinetic energy, which results in the formation of bonding and antibonding minority-spin levels in the alloy. The vanadium sites then have more spin-down electrons than spin-up electrons, resulting in a moment anti-parallel to that of the Fe, i.e. FeV is a ferrimagnet. Overall, however, the total number of spin-up electrons is in the majority, until the moments collapse at $c \approx 0.30$. This collapse of magnetism in the V-rich alloy is easily understood in terms of the reduction of the Fe-induced exchange-splitting of the V sites as the number of Fe neighbors is reduced. Of course, the exact occurrence of the collapse of magnetism depends on a delicate balance of bonding and exchange. As for the majority levels, they are well separated in energy and therefore can only form split bands, i.e. mostly all Fe or all V in character. One physical ramification is that the minority electrons will be able to hop to any neighbor, while the majority electrons will be confined to one species. This simplified picture cannot be taken too literally since it can not reproduce the small maximum in the iron moments as a function of concentration, see Fig. 3a., which is caused by a subtle interplay between moments and bonding.

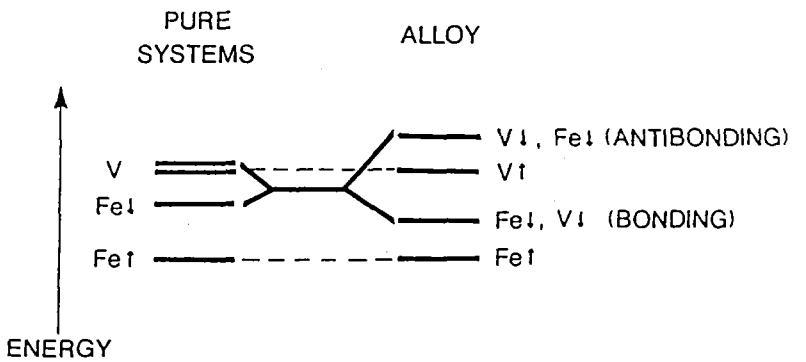

Fig. 2. A schematic (tight-binding) picture of the microscopic levels for Fe and V before alloying and BCC FeV alloys after alloying.

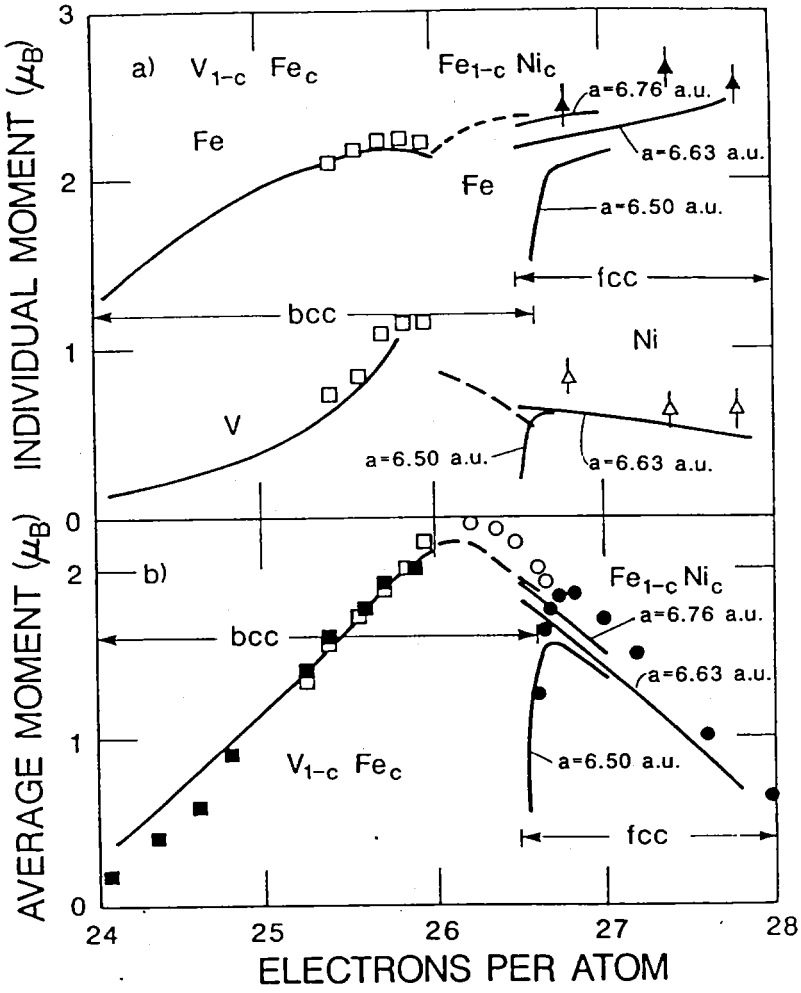

Fig. 3. The a) individual moments and b) average moments of FCC and BCC Ni_cFe_{1-c} alloys and BCC Fe_cV_{1-c} alloys plotted as a function of electron-to-atom ratio. The calculations are denoted by the solid (FCC) and dashed (BCC) lines. The experimental data are plotted as the other symbols (see Ref. 14 for details and references to the original experiments).

From this simple picture we can infer what the electronic density of states (DOS) should be. Since the Fe and V majority (spin-up) d-states are well separated in energy, we expect a very smeared majority DOS resulting from the large disorder that the majority electrons 'see ' as they travel through the lattice. On the other hand, the minority (spin-down) electron DOS should have sharp peaks associated with the lower energy, bonding states and the higher energy, antibonding states. In Fig. 4, the KKR-CPA calculated electronic density of states for $Fe_{0.50}V_{0.50}$ is shown (**14**). Note that the majority DOS is very smeared due to disorder, and the minority DOS is much sharper with the bonding states fully occupied and the antibonding states unoccupied. The vertical solid line indicates the Fermi level, or chemical potential, of the electrons, below which the states are occupied. It is worth stating that the simple picture given above was constructed from hindsight. In general, the DOS depends on the underlying symmetry of the lattice and the subtle interplay between bonding and magnetism.

As an example of our agreement with experiment and the charge self-consistency procedure, we have calculated the variation of the local magnetic moments versus concentration for NiFe and FeV alloys and have reproduced (**14**) the Slater-Pauling curve, as shown in Fig. 3b. For example, in the BCC FeV system, for a wide range of concentrations, the Fermi level is trapped in a valley between bonding and antibonding states in the minority-spin electron density of states. The linear dependence of the magnetization as vanadium is added to iron (with less than 70% vanadium) is then a result of adding electrons to the majority-spin states. For FCC NiFe alloys, before the moments collapse in the iron-rich alloys (see Section 4c-d.), we see that the moments vary in a nearly linear fashion. From the FCC nickel-rich end, this linear behavior is a result of a

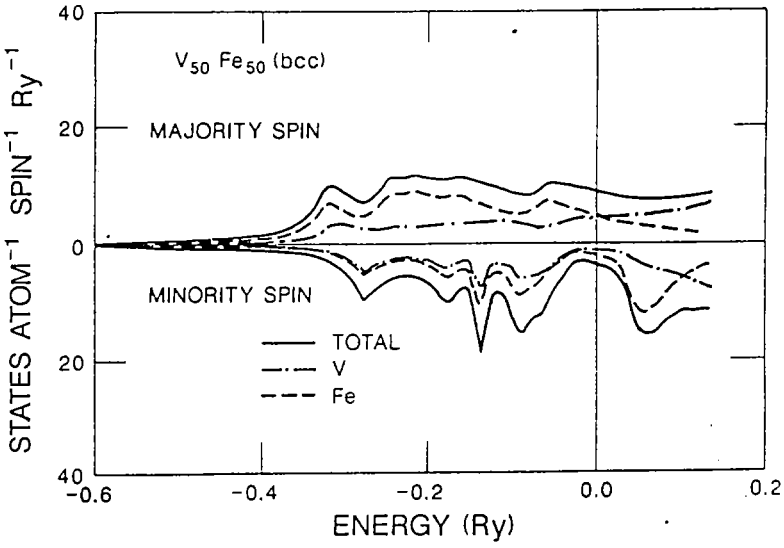

Fig. 4. The density of states per atom per Rydberg unit for BCC $Fe_{0.50}V_{0.50}$.

filled majority-spin electron DOS, which we shall discuss in Section 4d. This feature fixes the number of spin-up electrons, and therefore, as iron is added to nickel, the electrons are removed from the spin-down states increasing the moment.

In FCC NiFe alloys, as we shall see, if magnetism is neglected, there would be no decrease in the lattice constant due to a collapse of moments in the INVAR region and, hence, no INVAR effect. Magnetism is the essential ingredient and, since the majority d-band is full, the minority electrons play a significant role in determining many of the physical properties. By contrast, it is the majority electrons in the FeV alloys that play the more significant role. This difference will have tremendous effects in other macroscopic properties, as we shall shortly discover. It should also be obvious that changes in the local chemical environment can have dramatic effects on the magnetism, especially in systems which change the local environments rapidly, such as occurs in multilayers. For example, in the Fe-rich FeV alloys the exchange-splitting on the vanadium sites is induced by the Fe sites, and, as the number of Fe atoms decrease, the magnetization vanishes. We shall discuss this topic briefly for the case of FCC NiFe alloys in Section 4b.

4. RESPONSE FUNCTIONS: THEORY vs. EXPERIMENT

The theory of the energetics of random alloys at zero temperature is an initial step in the understanding of alloy stability. However, as suggested in the Introduction, we are interested in alloys at finite temperature, primarily because 1) the higher the temperature, the more important entropy becomes, forcing one to address the disordered state; 2) most materials processing takes place at high temperatures; 3) an investigation of the high-temperature, disordered state can reveal which type of short-range order (SRO), chemical and/or magnetic, is favored. To proceed, we cannot be satisfied with zero temperature band theory applied to ordered metals, but must develop finite temperature techniques suited to disordered alloys. Obviously, construction of first-principles phase-diagrams is a compelling area of study. Equally important is the impact that SRO may have on mechanical and physical properties. This problem can be conveniently divided into understanding the origin of the ordering and the effects that they may have on the physical properties. Moreover, the "driving forces" responsible for the SRO in the disordered state usually persist to lower temperatures where they determine the stability of various possible long-range ordered structures. In this paper, we are only going to concern ourselves with the mechanisms responsible for and the prediction of chemical (magnetic) SRO in NiFe alloys and the effects of chemical SRO on the local magnetic moments in this alloy.

4a. MAGNETIC FLUCTUATIONS

In magnetic systems, above the transition temperature, it is possible for local moments to exist, but with their directions oriented so as to produce no net magnetization. For this to occur the electrons of either spin hop from site to site with sufficient correlation that the moments are maintained over a "long" time. The concept of different time scales is required for moments to form; that is, magnetic correlation exists for time scales longer than the hopping time and shorter than the characteristic spin-wave frequency of the system. In Fe and its alloys, this is the case. The so-called disordered local moment (DLM) state **(15)** in which all the local moments are uncorrelated and randomly oriented from site to site, is one possible description of the high-temperature, paramagnetic state. In the case of BCC Fe, for example, one can see that we have a system analogous to a random, binary alloy, where up (down) moments are the A(B) species. We only note in passing that it is possible to map **(8)** the three dimensional disordered moments to a Ising-like (up,down) moment picture, but only above T_C.

Since we wish to compare our theory with experiment, it is appropriate to calculate quantities that may be compared directly. For magnetic systems, neutron scattering experiments provide direct probes into the underlying interaction of the systems, since they measure the moment pair correlation functions. For example, in real space, the magnetic susceptibility for an elemental magnet is given by

$$\chi_{ij} = \langle \mu_i(\hat{e}_i)\mu_j(\hat{e}_j)\rangle - \langle \mu_i(\hat{e}_i)\rangle\langle \mu_j(\hat{e}_j)\rangle \quad , \tag{2}$$

where $\mu(\hat{e}_i)$ represents the moment at the site i with orientation $\hat{e}_i$. The brackets, <...>, indicate thermal averaging. Approaching the transition temperature, T_C, from the high-temperature, uncorrelated state, this function will become non-zero, indicating that correlations exist between the orientation of the moments in the system and, thus, the onset of magnetic order.

Thus, using the KKR-CPA which allows us to average over the magnetic disorder in a mean-field approximation, we may work out the thermal average in this high-temperature, disordered state; we find **(8,15)**

$$\chi(\underline{k}) = \frac{(1/3)\beta C(T)}{1 - (1/3)\beta I^{(2)}(\underline{k})} \quad , \tag{3}$$

where $\chi(\underline{k})$ is the lattice Fourier transform of χ_{ij} and $I^{(2)}(\underline{k})$ is that of the direct correlation function defined by

$$I^{(2)}_{ij} = \left(\frac{\partial^2 \langle \Omega(\{m_i\})\rangle}{\partial m_i \partial m_j}\right)_{m_i = \bar{m} = 0 \text{ for all } i} , \tag{4}$$

where $\beta = (k_B T)^{-1}$ is the inverse temperature, and $m_i = \langle \mu_i(\hat{e}_i) \rangle$ is the local site magnetization, which above the transition temperature must be zero. At the transition temperature, $\chi(\underline{k})$ diverges, indicating the onset of magnetic order. The particular vector $\underline{k}$ at which $\chi(\underline{k})$ diverges determines the type of magnetic order. The coefficient C(T) is known as the Curie constant for Heisenberg magnets. As a simple example, if the magnetic system were described by a simple, rigid-moment, Ising-model Hamiltonian (i.e., $H = -\Sigma_{ij}\ J_{ij}\ \mu_i\ \mu_j$), where moments are either oriented up or down ($\hat{e}_i = \pm 1$), then $I^{(2)}(\underline{k})$ would just be the Fourier transform of the phenomenological exchange interactions J_{ij} (i.e., a magnetic, pairwise ordering energy). Most importantly, a central result of the theory is that the quantity $\Omega(\{m_i\})$ is the average of the electronic grand potential for each configuration $\Omega(\{\hat{e}_i\})$ and contains all the underlying electronic structure (interactions) within the LDA-KKR-CPA approach. Since the theories of magnetism and alloys may be mapped into one another, we make a few other

comments in regard to the NiFe alloys in the next section on alloy chemical short-range ordering.

Staunton, *et al.* (15) have performed such a calculation on BCC Fe and obtained $T_C \approx$ 1280 K, compared to 1040 K for experiment (16). Recall that only the atomic number of Fe was an input to that calculation. Moreover, they predicted a collapse of the exchange-splitting along certain k-direction. This has since been seen by spin-polarized photoemission experiments. We refer the reader to the paper of Staunton, *et al.* for further details and other comparisons to experiment. So this theory of magnetic phase transformation is qualitative, quantitative, and predictive!

Before addressing the problem of both chemical and magnetic fluctuations in the FCC NiFe alloys, it is helpful to understand the behavior of pure FCC Fe. Although FCC Fe only exists at high-temperatures, it is instructive to investigate the moments and the character of their interactions in this system, and how these might relate to the alloys. In Fig. 5, we have reproduced the calculated moments for FCC Fe as a function of lattice constant (or volume) for three different magnetic states: ferromagnetic (FM), disordered local moment (DLM) (4), and antiferromagnetic (AFM) states (17). For fixed large volumes, the FM state has large moments and is lowest in energy. At small volumes, the non-magnetic state is lowest in energy, and , in fact, is the global energy minimum. However, at intermediate volumes the AFM and DLM states have similar moments and energies, although, at 6.6 a.u., the moments in the DLM state collapse. These results suggest that the Fe-Fe correlations on an FCC lattice are extremely sensitive to volume, and change from FM to AFM as the volume is reduced.

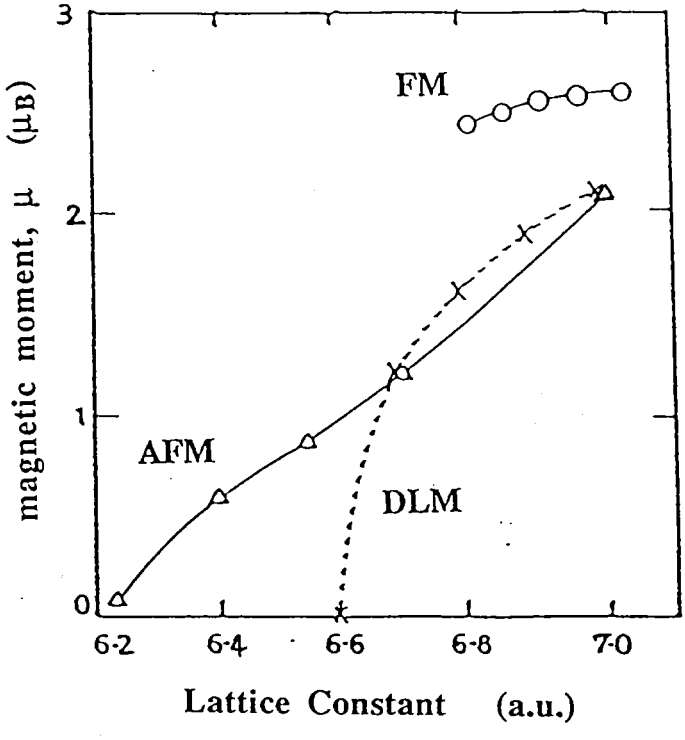

Fig. 5. The moments versus lattice constant calculated for FCC iron. The ferromagnetic (FM) and disordered local moment (DLM) calculation are from Pinski et al. (Ref. 4). The antiferromagnetic (AFM) results are from Wang et al. (Ref. 17) for the (100) AFM state.

In fact, our calculations of the high-temperature susceptibility (i.e., the moment-moment correlations) for various lattice constants (4) indicate that at large lattice constants a > 6.8 a.u. the correlations are FM. However, as the lattice constant is reduced from 6.8 to 6.7 a.u., the interaction change from FM to AFM in nature. Thus, the interactions between Fe moments on a FCC lattice indeed have a dramatic dependence on volume. It is then interesting to note that the NiFe alloys all have lattice constants in the range 6.5 < a < 6.8 a.u., where the magnetic correlations of pure Fe on an FCC lattice are changing.

These first-principles calculations give some credence to the speculation made in the Introduction that the nature of the Fe moment interactions are, or evolve into, AFM and as a result produce the various physical phenomena exhibited by NiFe alloys. As stated there, simple spin-only models do roughly reproduce the $\bar{\mu}$ vs. c and T_C vs. c curves if the Fe-Fe interactions are AFM, but give no insight into why this might be the case. It is the purpose of ab-initio calculations to determine, without bias, the underlying causes of these properties. Without performing a first-principles calculation of the high-temperature susceptibility for the NiFe alloy which incorporates both magnetic and chemical fluctuation on an equal basis, these results may only suggest the origin of the INVAR phenomena. In fact, in the region of $Ni_{0.35}Fe_{0.65}$, it will be very important to account for both types of fluctuations, since experimentally the Curie temperature (the temperature below which long-range magnetic order exists) is decreasing in this concentration range, and, as we will show in succeeding sections, the effect of magnetic order on the chemical fluctuation has profound effects in the NiFe alloys.

4b. CHEMICAL FLUCTUATION: SHORT-RANGE ORDER IN MAGNETIC ALLOYS

4b.1 CONCEPTS AND THEORY

Earlier in this paper we have focused our attention on the electrons, which, unlike the atoms, do not come in different species. It is the nuclei, due to differing number of protons, which distinguish individual types of atoms. To study SRO we move the nuclei to the forefront while relegating the electrons to a supporting role of modifying the interactions between nuclei. The motivation for this and the manipulations required to bring this about within the context of electronic structure calculations were given in the concentration fluctuation theory introduced by Györffy and Stocks (18). In this paper, we will assume that the more complete review of the theory given in Ref. 7 is known and only discuss the role that magnetism may play in alloy SRO and physical properties. For this purpose, one must realize that really there are two kinds of electrons, spin-up and spin-down. How does this change the interaction between the nuclei and, thus, affect the SRO? We will specifically investigate these effects in the alloy $Ni_{0.75}Fe_{0.25}$.

The approach of Györffy and Stocks readily generalizes to the cases of alloys, such as $Ni_{0.75}Fe_{0.25}$, in the ferromagnetic state (8). The theory has two parts: the first part deals with the statistical mechanics of the alloy configurations in the mean-field approximation; the second part implements the first part on the basis of a spin-density functional description of the electronic energies for each configuration.

In this section, we restrict our attention to the study of the pair correlation functions, α_{ij}, also known as the Warren-Cowley short-range order parameters. In terms of the site occupation variables $\{\xi_i\}$, which take on the values 1 or 0 if the ith site is occupied by an A or B atom, respectively, the correlation functions are defined by

$$\alpha_{ij} = (< \xi_i\xi_j > - < \xi_i > < \xi_j >)/c_i\,(1-c_j) \qquad (4)$$

where the site concentrations are given by $c_i = < \xi_i >$. (The concentrations in the alloy problem are analogous to the magnetization in the magnetic problem). In the completely disordered state, all sites are equivalent ($c_i = \bar{c}$ for all i), and uncorrelated; thus, $\alpha_{ij} = 0$. At lower temperatures, SRO will result in the pair correlations taking on oscillatory values for the onset of LRO and the value 1 for the onset of clustering (phase separation).

Working out the thermal average in the mean-field approximation and in the disordered state, we find (8,18)

$$\alpha\,(\underline{k}) = \frac{2}{1-\beta c(1-c)\,S^{(2)}\,(\underline{k})} \quad , \qquad (5)$$

where $\alpha(\underline{k})$ is the lattice Fourier transform of α_{ij} and $S^{(2)}(\underline{k})$ is that of the direct correlation function defined by

$$S^{(2)}_{ij} = \left(\frac{\partial^2 <\Omega(\{c_i\})>}{\partial c_i \partial c_j} \right)_{c_i = \bar{c} \text{ for all } i} . \tag{6}$$

It is a central result of the theory that the quantity $\Omega(\{c_i\})$ is the average of the electronic grand potential for each configuration $\Omega(\{\xi_i\})$ over the inhomogeneous product distribution, which for an alloy is given by

$$P_i(\{\xi_i\}) = \prod_i P_i(\xi_i) , \tag{7}$$

where

$$P_i(\xi_i) = \begin{pmatrix} c_i & \text{if} \quad \xi_i = 1 \\ 1 - c_i & \text{if} \quad \xi_i = 0 \end{pmatrix} \tag{8}$$

The above thermodynamic averaging is a mean-field approximation. Since the CPA is based on this type of probability distribution, we use the KKR-CPA to evaluate $\Omega(\{c_i\})$ in the second, electronic part of the theory so as to be consistent with the mean-field approximation used in the thermodynamic averaging. Thus, the grand potential contains all the underlying electronic interactions, in complete analogy with the magnetic fluctuations discussed in the previous section.

To simplify matters, we consider first a theory at temperatures T above the chemical ordering temperature T_o (~780 K for $Ni_{0.75}Fe_{0.25}$) but below the Curie temperature T_c (the magnetic ordering temperature, ~870 K). That is to say, we are assuming that there are no magnetic fluctuations, the system is fully magnetized as in its ground state and is described by our spin-polarized SCF-KKR-CPA (**13,19**) but the local occupation numbers $\{\xi_i\}$ are allowed to undergo normal thermal fluctuations.

It is fairly straightforward to derive, formally, an inhomogeneous version of the spin-polarized SCF-KKR-CPA. It is inhomogeneous in the sense that on every site the CPA equations must be solved to determine the local non-equilibrium concentrations c_i. This implies a definite expression for $\Omega(\{c_i\})$ and, therefore, for the derivatives in eq. (6). When, in this expression, c_i is set equal to $\bar{c}$ for all i, we obtain a response function of the homogeneous spin-polarized SCF-KKR-CPA which may be evaluated numerically.

The details of the theory may be found in Ref. 8. Here we shall make only two general comments before moving on to the presentation of our results. First, we observe that $<\Omega>$ depends not only on the local concentrations $\{c_i\}$ directly, as in the non-magnetic theory of Györffy and Stocks, but also indirectly through the local moments $\{\mu_i\}$ which arise in the spin-polarized theory for each configuration. As a consequence $S^{(2)}$ consists of three contributions. For α = A or B, and in terms of the local chemical potential, defined as

$$S^{(1)}_i = \frac{\partial <\Omega>}{\partial c_i} ,$$

$$S^{(2)}_{ij} = S^{c,c}_{ij} + \sum_l S^{c,\mu^A}_{il} \gamma^A_{lj} + \sum_l S^{c,\mu^B}_{il} \gamma^B_{lj} , \tag{9}$$

where

$$S^{c,c}_{ij} = \left(\frac{\partial S^{(1)}_i}{\partial c_j} \right)_{\{\mu_i\}} ; \quad S^{c,\mu^\alpha}_{ij} = \left(\frac{\partial S^{(1)}_i}{\partial \mu^\alpha_j} \right)_{\{c_i\}} \tag{10}$$

$$\gamma_{ij}^{\alpha} = \frac{\partial \mu_i^{\alpha}}{\partial cj} \quad . \tag{11}$$

As a simple example, if there were no moments and the system were described by a simple, pair-wise interacting lattice gas model in the random-phase approximation, eq. (5) would be the Krivoglaz-Clapp-Moss formula and $S_{ij}^{(2)}$ would be $V_{ij} = \upsilon_{ij}^{AA} + \upsilon_{ij}^{BB} - 2\,\upsilon_{ij}^{AB}$ (the pairwise interchange energy), where $\upsilon_{ij}^{\alpha\beta}$ is a self-explanatory notation for the various interactions involved. For a lattice gas model with aligned, rigid moments interacting through phenomenological exchange interactions $J_{ij}^{\alpha B}$, $S_{ij}^{(2)} = S_{ij}^{cc} = V_{ij} + J_{ij}^{AA} + J_{ij}^{BB} - 2\,J_{ij}^{AB}$. Thus, $S_{ij}^{(2)}$ can be interpreted as an effective pairwise ordering energy modified by the presence of rigid moments. Evidently, γ_{ij}^{α} measures the effect of the chemical environment on the α moments at site i, and, hence, a quintessentially nonrigid moment effect!

As was the case for the susceptibility $\chi(\underline{k})$ in the last section, both $\alpha(\underline{k})$ and $\gamma(\underline{k})$ may be measured in spin-polarized neutron diffraction experiments **(20,21)**, where $\gamma(\underline{k})$ is the concentration weighted sum of the Fourier transforms of the γ_{ij}^{α}. That is, for neutrons polarized (anti-) parallel to the magnetization, $\varepsilon = \pm 1$, the cross-section per atom may be written as

$$\frac{d\sigma}{d\Omega}\Big)_{\varepsilon} \sim \chi(\underline{k}) + \varepsilon\alpha(\underline{k})\,\gamma(\underline{k}) + \alpha(\underline{k}) , \tag{12}$$

where the three terms are due to the magnetic-magnetic, nuclear-magnetic, and nuclear-nuclear correlations, respectively. The second term in eq. (12), which is due to the effects of cross-correlation, may be extracted by measuring the scattering from both polarizations, i.e.

$$\Delta\frac{d\sigma}{d\Omega} \sim 2\alpha(\underline{k})\,\gamma(\underline{k}). \tag{13}$$

Note, $\gamma(\underline{k})$ is the magnetic-chemical response (i.e., the response of the magnetic moments due to changes in the local environment) of the entire system. Thus, for a binary alloy, it is given by $\gamma(\underline{k}) = \{\mu_A - \mu_B\} + c_A\,\gamma^A(\underline{k}) + c_B\,\gamma^B(\underline{k})$. If the A and B moments are substantially different, the first term in $\gamma(\underline{k})$ may be dominant in the measurements, swamping the subtle environment effects. On the other hand, if the moments are antiparallel and about equal in magnitude, the entire cross-correlation contribution will be coming from the (possibly small) environment changes. Moreover, although the theory for the $\gamma(\underline{k})$'s is only valid for small changes in the concentration, if one assumes that the theory is valid for larger changes (as if they varied linearly with concentration, for instance), the alloy moments as a function of chemical environment may be calculated simply from this response. In the next section, we will apply this approach in the $Ni_{0.75}Fe_{0.25}$ when the system goes through an order-disorder transformation.

The next comment is technical and concerns the fact that $\langle\Omega\rangle$ is conventionally split into a single-particle contribution (related to the Green's function) and the so-called double counting corrections **(13,18)**. When taking the derivatives of the latter, as required by eq. (6), we have taken into account the local change in the magnetic moments only and neglected the local charge fluctuations with the environments. For NiFe alloys, the small charge transfer found in our SCF-KKR-CPA calculations validates the neglect of charge fluctuation terms.

4b.2 ORDERING IN $Ni_{0.75}Fe_{0.25}$

Recall that the high-temperature, chemically disordered state has the symmetry of the underlying lattice. Thus, the concept of a Brillouin zone is still valid. Depending on the temperature and where $S^{(2)}(\underline{k})$ has its global maximum, $\alpha(\underline{k})$ will diverge indicating an instability to some type of short range order. The particular type of SRO depends on the vector $\underline{k}$ at which $\alpha(\underline{k})$ diverges. For example, for a FCC lattice, a divergence at $\underline{k}$=(000) indicates a clustering tendency; whereas, a divergence at $\underline{k}$=(100) signals the onset of a Cu_3Au-type ($L1_2$) ordering. In Fig. 6, for $Ni_{0.75}Fe_{0.25}$ we show the $S^{(2)}$ (only the implicit moment dependence $S^{c,c}$ is shown) in the various directions in $\underline{k}$-space. It rises as k varies from $\underline{k}$= (000) to the zone boundary with a maximum at $\underline{k}$=(100). Thus, the theory predicts ordering with an $L1_2$ symmetry. Experimentally, $Ni_{0.75}Fe_{0.25}$ orders at around 780 K into the $L1_2$ structure (1). From our calculation, the divergence occurs for a temperature of 450 K. Although this is only 60% of the experimental ordering temperature, the explicit moment enhancement of $S^{(2)}$ has not been included. A calculation which includes the explicit moment enhancement effects is currently being performed and should bring the calculated transition temperature into closer agreement with experiment. It is also possible that the neglect of magnetic fluctuations is not entirely valid, since in the NiFe alloys the measured Brillouin curve deviates markedly from the ideal.

To examine the effects of magnetism, we have repeated the calculation for the alloy as a Stoner paramagnet (8); that is to say, we implemented the non-spin-polarized theory of Ref. 20. The peak then occurs for $\underline{k}$=(000) (see Fig. 6) and therefore indicates a clustering tendency -- or phase separation. In fact, the calculation suggested a very strong clustering tendency occurring at approximately 1500 K, which implies that the ordering tendency is entirely of magnetic origin!

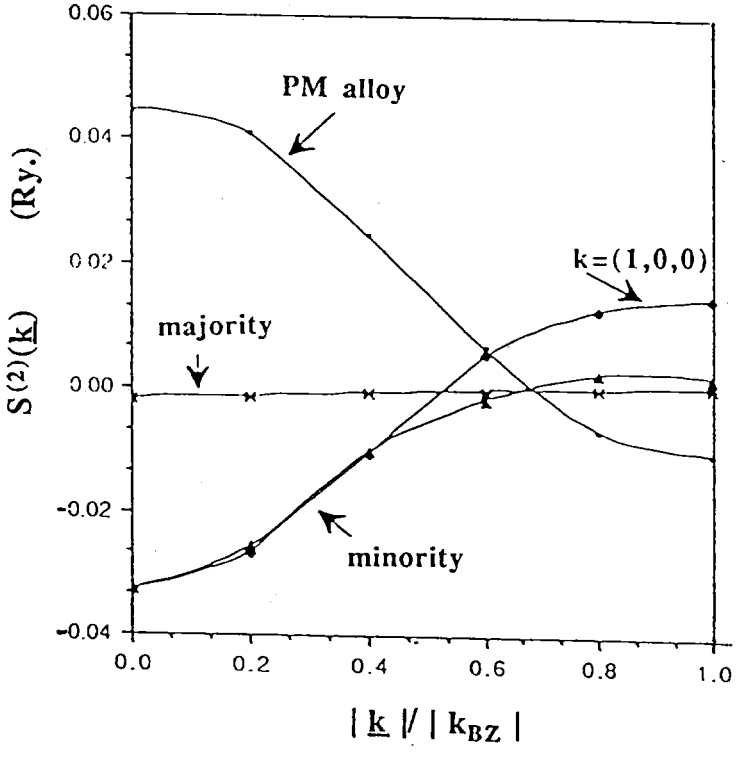

Fig. 6. $S^{(2)}(\underline{k})$ (in Rydberg units) vs. $\underline{k}$ is shown from the Γ to zone boundary points. The results do not include the explicit effects from moment enhancements, see text. For the ferromagnetic (FM) cases, the contributions from majority- and minority-spin electrons are shown separately. The FM minority contributions are shown along two k-vectors, so as to indicate the global maximum which is marked $\underline{k}$ = (1,0,0). The other curve which peaks at the zone edge is along the $\underline{k}$ = (1,.5,0) direction. For the paramagnetic (PM) case, all directions in k-space all contribute roughly equally; thus, only the $\underline{k}$ = (1,0,0) direction is plotted.

4b.3 WHAT DRIVES THE ORDERING PROCESS?

To understand the above phenomenon of clustering in the paramagnetic state but ordering in the ferromagnetic state, we recall some general features of the electronic forces for order and disorder in metallic alloys. In transition metal alloys where the d-band is roughly half- filled, ordering is expected. Under such circumstances, only bonding states are filled and the bonding states of the ordered metal are lower than those of the disordered state due to level repulsion. On the other hand, almost completely filled or empty bands can be expected to lead to clustering. A modern discussion of the rules has been given by Heine and Sampson (22).

As can be seen by inspecting Fig. 7, the d-band is almost completely filled in the paramagnetic state. Accordingly, clustering is expected in agreement with the prediction from our calculation of the direct correlation function $S^{(2)}$.

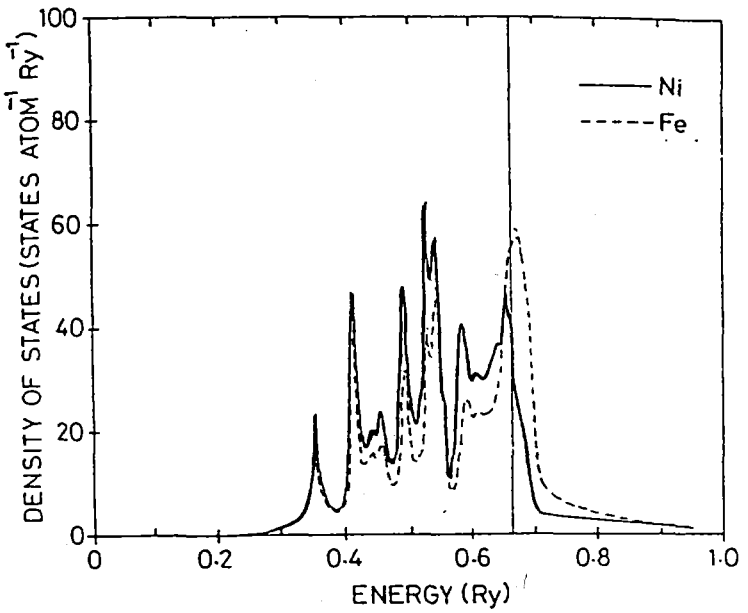

Fig.7. Average partial d-electron density of states are shown for paramagnetic FCC $Ni_{0.75}Fe_{0.25}$. The solid (dashed) lines are the nickel (iron) contribution. The solid vertical line is the Fermi level and the energy zero is with respect to the majority muffin-tin zero.

However, when the bands are exchange split due to magnetism, the majority band is completely filled, see Fig. 8. Such filled bands are relatively neutral with respect to compositional ordering. They are particularly ineffective in this case because, as was discovered by Johnson et al. (19), the majority electron states have very long lifetimes, indicating that the majority electrons "see" roughly the same potentials on the Ni and Fe sites; i.e., the electronic energy levels for the majority electrons are very close in energy and electrons cannot distinguish between a Ni or Fe site. Indeed, we find that the majority spin electrons contribute negligiblely to $S^{(2)}$.

The tendency for short range ordering is then determined solely by the minority spin electrons. Upon exchange splitting, the majority d-bands are filled, whereas, the minority bands are more nearly half-filled. As suggested in Fig. 8, this shift apparently positioned the Fermi level in the density of states making the occupation sufficiently close to half filled, producing the ordering tendency.

Interestingly, at very high temperatures where magnetism is insignificant, the thermochemical data (23) also implies phase separation at low temperatures. Currently, this is the only experimental support for the above mechanism driving the compositional order in this alloy. Further experimental confirmation will be needed before it can be firmly established that the compositional ordering is entirely of magnetic origin.

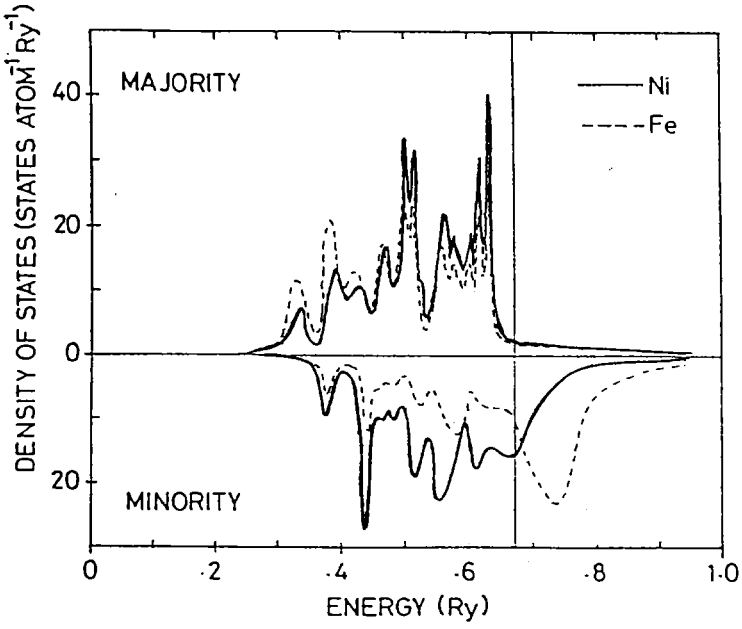

Fig. 8. The same as in Fig. 7, but for the ferromagnetic FCC $Ni_{0.75}Fe_{0.25}$.

Finally, we note that the moment-chemical response functions, $\gamma(\underline{k})$, that we have discussed above briefly refer to the nonrigid, itinerant nature of the moments and, thus, the sensitivity of the moments to chemical environment changes. The Fourier transform of $\gamma(\underline{k})$, γ_{ij}^{α}, has a particularly revealing physical interpretation. These quantities describe the change in the size of the moment on a site i in the lattice if it is occupied by an α =A(B) atom and if the probability of occupation is altered on another site j. Having calculated $\gamma_{ij}^{A(B)}$, we can study the moments as a function of chemical environment using the relation

$$\mu_{\alpha,i} = \mu_{\alpha}^{cpa} + \sum_{j} \gamma_{ij}^{\alpha} \Delta c_j \quad , \tag{14}$$

where the first term is the moments calculated for the random alloy, and the second term is the change in the local moments due to a change in the local concentration, or number of A(B) atoms. For instance, with an environment consistent with ordered Ni_3Fe, we find the average moment increases by 5% compared to the disordered state, which agrees with experiment (19).

Notably, these sorts of calculations may be especially interesting as an aid to experiment and in the design of novel magnetic alloys. For example, one may investigate multilayers, which we have done for FeV, with very good agreement with experiment, see Ref. 24.

4c. MAGNETIC AND CHEMICAL DISORDER: THEIR ROLE IN THE INVAR PHENOMENA

Thus far we have discussed the magnetic susceptibilty of FCC Fe, which revealed a great sensitivity to volume, and the short-range order in Ni-rich NiFe alloys, which was driven by the ferromagnetism. In this section, we focus on the INVAR concentration range, in particular, chemically disordered, FCC $Ni_{0.35}Fe_{0.65}$, and investigate the relative stability of various magnetic phases. Traditional band-structure techniques have not been able to investigate this alloy due to the chemical disorder. But, as we shall see below, magnetic disorder also becomes relevant, further disabling the use of these methods. Not only may we account for both effects, but our total energy capability allows a preliminary investigation of this alloy at T=0 K, with some suggestions as to the finite temperature behavior.

The results of T = 0 K total energy calculations for the ferromagetic (FM), disordered local moment (DLM), and nonmagnetic (PM) states are shown in Fig. 9. These three magnetic states may, or may not, be energetically favorable in the INVAR region. Of course, there are perhaps AFM and spin-glass phases that will also be possible, however, the DLM state contains antiparallel moments and should be a good approximation to these other states. At some finite temperature, though, the DLM state, with such a large entropy, will have the lowest free energy if it is close to being the lowest energy state at T= 0 K. It is worth repeating here that, for Ni concentrations greater than 50%, the FM state is the lowest energy state by a large margin and determines the properties of the Ni-rich alloys.

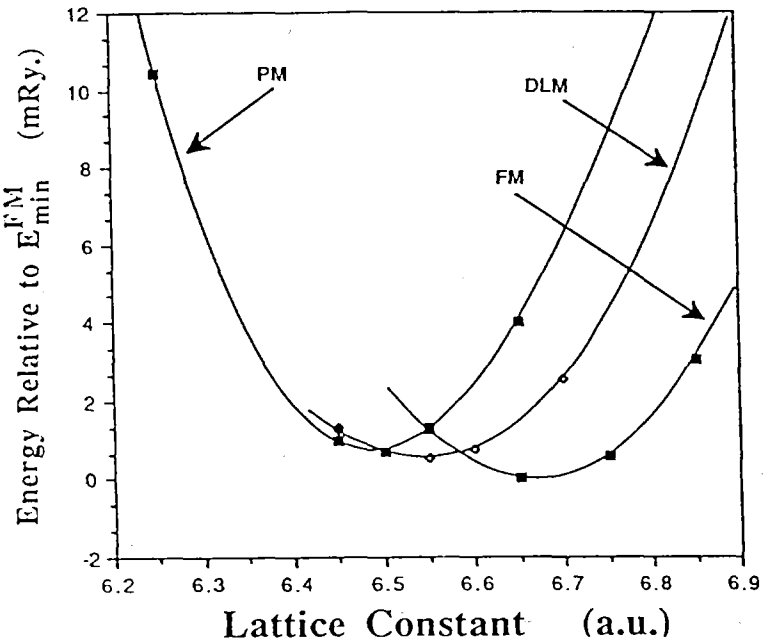

Fig. 9. The T = 0 K total energy for FCC $Ni_{0.35}Fe_{0.65}$ for three magnetic states, FM, DLM, and PM. The energy plot is relative to the FM energy minimum, i.e. E= -2693.90718 Ry.

At this concentration, the equilibrium lattice constants are 6.66, 6.54, and 6.48 a.u., for the FM, DLM, PM states, respectively. Several comments are in order. First, at this concentration the FM state is the lowest energy state by 0.54 mRy. over the DLM state, in contrast to several mRy in the Ni-rich alloys. (Note, 1 mRy ≈ 158 K.) However, a small increase in the Fe concentration makes the DLM state lower in energy. Upon further increase in the Fe content (≈ 70% Fe), the DLM and the PM states are almost degenerate and lower than the FM state. As a result, the lattice constant of NiFe in this concentration range will decrease with increasing Fe content, as is observed, and the moments collapse. Second, as the temperature is raised, the DLM state would have the lowest free energy and so the volume and moment will be sensitive to the temperature, which is the case. Third, since the DLM state (which has unaligned moments) is lowest in energy in the range $0.30 < c_{Ni} < 0.35$, antiparallel arrangements of Fe moments are not very energetically unfavorable, which is supported by spin-polarized neutron scattering (21). Fourth, the small energy differences between these various magnetic states imply a sensitivity of the magnetization to any applied field. Indeed, in the INVAR region there is a very large susceptibility enhancement. Fifth, a naive estimate of the free energy of the DLM suggests that the FM state is unstable at T ≈ 60 K. It is interesting that a.c. susceptibility measurements (25) imply that INVAR is a reentrant spin-glass at T ≈ 40 K. Our results are similar to those of Kakehashi (26), who uses a less sophisticated model of the electronic structure and stresses the need to go beyond the CPA by treating local environment effects. We stress, however, that in our calculations we have used an "averaged" environment, i.e. the effective CPA medium, and found it unnecessary to invoke large environmental effects to obtain our results. On the other hand, our calculation are only at the level of mean-field theory and as such will not correctly describe critical behavior (where fluctuations in the local environment dominate) and, therefore, will not give the exact critical concentration at which the moments collapse.

The calculate moments for the FM state are $\mu^{Fe} = 2.40\ \mu_B$ and $\mu^{Ni} = 0.64\ \mu_B$ ($\bar{\mu}$= 1.78 μ_B), with a negative polarization between atoms; all of which is in good agreement with experiment (21). The Fe moments above T_C, as given by the DLM calculation, are $\mu^{Fe} = 1.42\ \mu_B$. For $T_C < T < 2T_C$, neutron scattering experiments (27) obtain an $\mu^{Fe} = 1.40\ \mu_B$. At both low and high temperatures, the moments are in agreement with experiment. Because the Fe moments decrease by 40%, and the Ni moments by 100%, as T approaches T_C from below, the ordering tendency should be decreasing with increasing T since the magnetism is diminishing rapidly with increasing Fe concentration or temperature, which was not the case in the Ni-rich alloys. This could explain the geological time scale with which these alloys order in the INVAR region. A calculation of the short-range order parameter, $\alpha(\underline{k})$, in which both the magnetic and chemical disorder are accounted for, is planned to substantiate this suggestion.

In previous theories of INVAR, a number of different mechanisms have been invoked to explain the many anomalous properties of these types of alloys, for example, the 2-γ hypothesis (28) (which assumes two microscopic energy levels in FCC Fe); the transition from strong to weak ferromagnetism (29); concentration fluctuations (30) which produce macroscopically different magnetic regions; volume fluctuations (31) which produce microscopically different magnetic regions. Except for volume fluctuations, all the other possibilities are included within our calculations without bias. Our calculations show that all the above mechanisms play a role. However, the most important features necessary are 1) a large, sharp DOS just below the Fermi level, which leads to a dramatic dependence of the magnitude of the moments to the position of the Fermi level, and 2) the Fermi level is sensitive to the degree of alignment of the moments, which is altered by thermal effects. This is unlike the traditional notion of a strong to weak FM transition.

It is worth pointing out that chemical disorder plays only a subsidiary role in this explanation; only the large DOS feature at the Fermi level and the subsequent crossover to a magnetically disordered state are necessary. This would allow a similar scenario to occur in the Fe_3Pt INVAR alloy, which is chemically ordered. We note that Kisker et al. (32), in their recent spin-polarized photoemission experiments on Fe_3Pt, analyzed their results by considering only two macroscopic, magnetic states (FM and PM) and interpreted this to support the 2-γ hypothesis. However, as shown by Kakehashi (33) using our FCC Fe DLM results, the presence of a magnetic disordered state in Fe_3Pt is in better agreement with experiment.

4d. CONCENTRATION DEPENDENCE OF NiFe PROPERTIES

There are many alloy properties which one may investigate as a function of composition. As such, we discuss here only the moments, lattice constant (volume), specific heat coefficient, and residual resistivity versus concentration, c, of Ni: $\bar{\mu}$ vs. c, a vs. c, γ vs. c, and ρ_{res} vs. c, respectively. The latter two topics will be discussed only qualitatively. These quantities have not been specifically chosen for favorable comparison, but just as an indication of what should be expected. For example, it is possible to calculate the hyperfine fields for random alloys which may be measured by Mößbauer experiments. For the FCC NiFe alloys, these calculations (34) are in good agreement with experiment, with correct trends and roughly 10-20% errors. In fact, they indicate that in some instances experimentalist may be incorrectly analyzing their data, since they neglect contributions to the hyperfine fields past one nearest-neighbor shell and theory indicates there are significant contributions up to the fifth nearest-neighbor shell.

In Fig. 3, we presented calculated moments of both Fe and Ni in the FCC and BCC structure, which agreed well with the experiment. As is apparent from the FCC DOS plotted in Fig. 8, the majority electron d-bands are filled in the Ni-rich alloys, and the majority electron DOS at the Fermi level, ε_F, is small. Thus, upon alloying Ni with Fe, the electrons are removed from the minority d-bands which at ε_F has the larger DOS. This depletion of minority electrons with increasing Fe content results in a linear increase in the net moment. At some concentration the above picture breaks down and electrons with both spins will be affected. The Fermi level will enter the majority d-bands, which, because of the large, sharp DOS, results in a drastic decrease in the net magnetization - the INVAR moment collapse. In particular, most of the states in the top edge of the d-bands are Fe states and, therefore, the Fe moments decrease first.

In the INVAR region, when the Fermi level is just outside the majority DOS, any small decrease in the volume (more practically, an increase in the pressure) will result in such a depletion of majority electrons, hence, the observed sensitivity of the moments to changes in the volume or pressure.

Also, as we have seen in the last section, the volume is reduced with increased Fe concentration with a concomitant collapse of the moments, hence, the deviation of a vs. c. The exact concentration that the moment collapse takes place may be slightly different than we calculate, since this depends on the critical fluctuations in the system which are only described approximately within the mean-field approach which we are using. Nevertheless, we describe the collapse in the correct region with, perhaps, an ever so slight shift to higher Fe concentrations than seen experimentally. The T=0 K extrapolated experimental bulk moduli in Mbars for Ni-50%, Ni-37.7%, Ni-35%, and Ni-33.6% are approximately 1.84, 1.40, 1.14, and 1.08, respectively -- extremely sensitive to variations of the concentration. The calculated T=0 K, ferromagnetic, bulk moduli for $Ni_{0.50}Fe_{0.50}$ and $Ni_{0.35}Fe_{0.65}$ are 2.21 and 1.80 Mbars, respectively. Even taking into account the usual 10-20% discrepancy, our calculated bulk moduli support the suggestion of a slightly shifted concentration dependence. The calculated bulk moduli for $Ni_{0.35}Fe_{0.65}$ in the DLM and PM states are 1.60 and 2.90 Mbars, respectively. With a small increase in Fe content, the DLM state becomes energetically favorable and, therefore, would futher decrease the bulk modulus. Albeit, we have a slightly shifted concentration dependence, the same sensitivity to concentration as seen in experiment is obtained from our calculations. We are currently performing calculations in the very narrow concentration range where the INVAR anomalies occur to obtain the exact concentration dependence given from the theory.

The concentration variation of the specific heat coefficient, γ, is easily obtained from the electronic structure. To see this, recall that γ is proportional to the DOS at the Fermi level (the number of states that are available for occupation), i.e. $\gamma \sim N(\varepsilon_F)$. In pure FCC Ni, ε_F lies in the large peak in the minority d-bands, and above the majority d-band within the top of the low DOS 4s-band. As Fe is alloyed with Ni the DOS structure changes, as is shown in Fig. 8. The DOS changes predominantly in the minority d-bands due to the disorder introduced by the large difference in the exchange-splitting from Ni and Fe, as we have discussed earlier. In Fig. 8, one can see that the disorder smears the minority DOS and allows mostly the Ni d-states to be occupied, leaving ε_F in a minimum in the DOS between the Ni and Fe minority d-states. Thus, we expect initially to see the specific heat coefficient decrease upon alloying with Fe. As we have mentioned in several instances, inevitably ε_F will enter the tail of the majority d-band and, as a result, the DOS will begin to rise and then dramatically increase when the large peak is encountered. This behavior of γ is experimentally the case for FCC NiFe alloys up to the INVAR regime.

The residual resistivity is a rather complicated quantity to calculate since it requires the determination of the scattering from occupied to unoccupied states at the Fermi level and, hence, the lifetimes of the electrons. The concentration dependence of the residual resistivity of NiFe alloys can be described as follows. Roughly speaking, s-electrons at ε_F are 'fast' electrons; on the other hand, d-electrons are rather localized (more atomic-like) and hence are characterized by a slower hopping rate from site-to-site, i.e. they are 'slow' electrons. Because disorder does not affect the electrons in the majority spin bands, the lifetimes and mean-free paths of these electrons will be large compared to those of the minority spin bands. Since the conductivity is proportional to the velocity and lifetimes of the electrons at ε_F, the majority electrons are almost entirely responsible for the large conductivity - small resistivity. With such a large mean-free path for the majority electrons, one finds the majority Fermi surface to be sharp and well-defined. Conversely, in the minority-spin scattering channel, the minority Fermi surface is smeared out due to the short mean-free path. This implies that environmental effects, such as due to clustering, will not affect the resistivity of the Ni-rich alloys. For pure Ni the residual resistivity is zero. Upon alloying Ni with Fe, the disorder in the minority channel increases the resistivity some, but the conductivity due to the majority-spin electrons limits the rise in resistivity. However, in the INVAR region when the Fermi level enters the majority d-band, the above picture is no longer valid. In this case, the resistivity increases dramatically since 1) there is a large change in the majority d-electron density of states, 2) the disorder in the majority-spin manifold increases, and 3) there is a change in the type of current carrier, i.e.

from faster s-like to slower d-like carriers. We plan to calculate the residual resistivity within the CPA for a quantitative comparison to experiment.

5. SUMMARY

We hope to have given you a concise but clear introduction into an area of first-principles approaches to the study of magnetic, disordered transition metal alloys, in particular, NiFe INVAR alloys. In summary, for T=0 K, the SCF-KKR-CPA provides an accurate means of investigating the energetics, magnetic and electronic structure of disordered alloys, just as traditional band-structure techniques do for ordered compounds. For $T > 0$, via a mean-field statistical mechanics approach, which uses the accurate KKR-CPA energy for the configurationally averaged energy and the ideal entropy only, we may investigate the underlying, atomic interactions responsible for the instability of the high-temperature, chemically disordered state to compositional ordering, the particular type of ordering, and the associated chemical ordering transition temperature. Moreover, the changes in alloy magnetism due to differing chemical environments are contained within the theory, allowing the study of the changes of the moments upon chemical ordering transitions, and, more generally, in multilayers. Because no adjustable parameters are required, the above theory is predictive and suggests underlying reasons for each behavior, which may be checked by experiment. The theory is quantitative since moments, lattice constants, bulk moduli, chemical ordering, etc., as a function of concentration agree well with experiment.

For the INVAR alloys discussed here, we have shown that magnetism is the all important ingredient for the various properties of these alloys. In particular, without magnetism the Ni-rich alloys would not chemically order, and, interestingly, the minority electrons are responsible for the ordering tendency. This prediction has yet to be confirmed by experiment. All features of these alloys thus far investigated, namely the $\bar{\mu}$, a, γ, and ρ_{res} vs. c and hyperfine fields, are explained within the above theory. In the INVAR region with increasing Fe content, the theory indicates that a crossover occurs from a state of magnetic order (ferromagnetism) to a state of magnetic disorder (such as the DLM state) and then finally to a non-magnetic state. This then is the underlying mechanism which produces the INVAR phenomena, and not the typical so-called strong to weak ferromagnetic transition; there is nothing overly mysterious, except a competition between several states instead of two. It is also quite possible that the collapse of magnetism on the FCC lattice gives rise to the $\gamma - \alpha$ martensitic phase transformation in the INVAR concentration range. We need to compare our present results with the magnetic, BCC NiFe energies in the INVAR region to investigate this conjecture, which is more problematic since comparison of different crystal structures is sometimes dubious in muffin-tin type calculations.

In the future, there are a number of avenues to explore, such as investigating the effect of impurities on short-range ordering and their influence on other alloy properties (essentially the ternary alloy problem). Furthermore, a generalization of the short-range ordering theory for magnetic alloys (8) has been derived which incorporates the fluctuation of moments that occur when an alloy is above its Curie temperature. This generalized theory will allow, for instance, the investigation of the competing interactions between magnetic order and chemical order in alloys at high temperatures, and how those interactions vary with concentration. Noting that theoretically the magnetic order was solely responsible for the short-range order in the Ni-rich NiFe alloys and that the ordering tendency in Fe-rich NiFe alloys is difficult to attain in normal metallurgical situations (e.g. it is only seen over geological time scales, such as occurs in meteorites) (35), our generalized theory will be used to address the suggestion that the change or reduction in magnetism (with either temperature or concentration variation) diminishes the tendency for short-range order in the FCC NiFe alloys near the INVAR concentrations.

ACKNOWLEDGEMENTS

Research at Sandia National Laboratories is supported by the U. S. Department of Energy, Office of Basic Energy Sciences Division of Materials Sciences. Also, DDJ received support in part from the NRC-NRL Research Associates Program and the computer resources

through the Pittsburgh Supercomputing Center. FJP acknowledges computer resources from both the Ohio and Pittsburgh Supercomputer Centers. Research at Warwick and Bristol is supported through the Science and Engineering Research Council of the U. K. Two of us (JBS and FJP) acknowledge partial support from a NATO research grant. The work at Oak Ridge National Laboratory is supported by the Division of Materials Sciences, U. S. Department of Energy under contract #DE-AC05-840R21400.

REFERENCES

[1] S. Chikazurin and C. D. Graham, Jr., Magnetism and Metallurgy, edited by A. E. Birkowitz and E. Kneller (Academic, New York, 1969) Vol. II, p.577.

[2] J. S. Kouvel, ibid., p. 523.

[3] e.g., E. I. Kondoskii and V. L. Sedov, J. Appl. Phys. 31, 331S (1960); and, T. Odagaki and T. Yamamoto, J. Phys. Soc. Jpn 32, 325 (1972).

[4] F. J. Pinski, J. B. Staunton, B. L. Györffy, D. D. Johnson, and G. M. Stocks, Phys. Rev. Lett. 56, 2096 (1986).

[5] Y. Kakehashi, J. Magn. Magn. Mat. 37, 189 (1983).

[6] H. Hasagawa, J. Phys. C 14, 2793 (1981).

[7] F. J. Pinski, D. M. Nicholson, W. H. Butler, G. M. Stocks, D. D. Johnson, and B. L. Györffy, Proceedings of the Third International Supercomputing Meeting, Boston, MA, May 15-20, 1988.

[8] J. B. Staunton, B. L. Györffy, D. D. Johnson, F. J. Pinski and G. M. Stocks, Alloy Phase Stability, eds. G. M. Stocks and A. Gonis, NATO-ASI Series B: Physics, (KLUWER Publishing, The Netherlands,1989); D. D. Johnson, J. B. Staunton, and B. L. Györffy (unpublished); for preliminary work see, J. B. Staunton, D. D. Johnson, and B. L. Györffy, J. Appl. Phys. 61, 3693 (1987).

[9] G. M. Stocks and H. Winter, The Electronic Structure of Complex Systems, editors P. Phariseau and W. M. Temmerman, NATO-ASI Series B: Physics, Vol. 113, Plenum Press, NY (1984).

[10] W. Kohn and L. J. Sham, Phys. Rev. 140, A1133 (1965).

[11] J. Korringa, Physica 13, 392 (1947); and, W. Kohn and N. Rostoker, Phys. Rev. 94, 11 (1954).

[12] P. Soven, Phys. Rev 156, 809 (1967).

[13] D. D. Johnson, D. M. Nicholson, F. J. Pinski, B. L. Györffy, and G. M. Stocks, Phys. Rev. Lett. 56, 2088 (1986).

[14] D. D. Johnson, F. J. Pinski, and J. B. Staunton, J. Appl. Phys. 61, 3715 (1987).

[15] J. B. Staunton, B. L. Györffy, G. M. Stocks, and J. Wadsworth, J. Phys. F 16, 1761 (1986).

[16] J. Crangle and G. M. Goodman, Proc. Roy. Soc. A321, 477 (1971).

[17] C. S. Wang, B. M. Klein, and H. Krakauer, Phys. Rev. Lett. 54, 1852 (1985).

[18] B. L. Györffy and G. M. Stocks, Phys. Rev. Lett. 50, 374 (1984).

[19] D. D. Johnson, F. J. Pinski, and G. M. Stocks, Phys. Rev. B30, 5508 (1984); and, D. D. Johnson, F. J. Pinski, and G. M. Stocks, J. Appl. Phys. 57, 3018 (1985).

[20] V. Pierron-Bohnes, M. C. Cadeville, and F. Gautier, J. Phys. F113, 1689 (9183).

[21] J. W. Cable and W. E. Brundage, J. Appl. Phys. 53 (1982).

[22] V. Heine and J. H. Sampson, J. Phys. F13, 2155 (1983).

[23] Ying-Yu Chung, Ken-Change Ksieh, and Y. Austin Chang, Metall. Trans. A17, 1373 (1986).

[24] D. D. Johnson, J. B. Staunton, and B. L. Györffy, to be published.

[25] T. Miyazaki, Y. Ando, and M. Takahashi, J. Appl. Phys. 57, 3456 (1985).

[26] Y. Kakehashi, J. Magn. Magn. Mat. 37, 189 (1983).

[27] M. F. Collins, Proc. Roy. Soc. 86, 973 (1965).

[28] R.J. Weiss, ibid. 82, 2811 (1963); and, for a similar based model, P. Chevenard, Rev. Metall. (Paris) 11, 841 (1914).

[29] D. M. Edwards and E. P. Wohlfarth, Proc. Roy. Soc. A303, 127 (1968).

[30] S. Kachi and H. Asano, J. Phys. Soc. Jpn 27, 536 (1969), and, ibid., pg. 542.

[31] G. P. Renaud and S. G. Steinemann, Physica B 149, 217 (1988). D. J. Kim, J. Appl. Phys. 55, 2347 (1984).

[32] E. Kisker, E. F. Wasserman, and C. Carbone, Phys. Rev. Lett. 58, 1784 (1987); and, Phys. Rev. B 35, 7760 (1987).

[33] Y. Kakehashi, (to be published).

[34] H. Ebert, H. Winter, B. L. Györffy, D. D. Johnson, and F. J. Pinski, J. Phys. F 18, 719 (1988).

[35] For current details see: these proceedings of the INVAR session of the The Metallurgical Society Meeting, Las Vegas, NV, 28 Feb-3 March, 1989.

UNLIMITED RELEASE
INITIAL DISTRIBUTION

U. S. Department of Energy
Office of Basic Energy Sciences
Attn: Iran L. Thomas
Washington, D.C. 20545

U. S. Department of Energy
Office of Basic Energy Sciences
Attn: R. Gottschall
Washington, D.C. 20545

U. S. Department of Energy
Office of Basic Energy Sciences
Attn: Richard W. Heckel
Washington, D.C. 20545

U. S. Department of Energy
Office of Basic Energy Sciences
Attn: L. C. Ianniello
Washington, D.C. 20545

U. S. Department of Energy
Office of Basic Energy Sciences
Attn: D. K. Stevens
Washington, D.C. 20545

U. S. Department of Energy
Office of Basic Energy Sciences
Attn: J. Darby
Washington, D.C. 20545

A.E.R.E., Harwell Laboratory
Attn: M. W. Finnis
Theoretical Physics Division
Oxfordshire, OX11 0RA, England

Alcan Aluminum Corporation
Attn: Dr. Frank V. Nolfi, Jr.
124 Mt. Auburn Street
Cambridge, MA 02138-5701

Alcoa Technical Center
Alloy Technology Division
Alcoa Laboratories
Attn: Barbara O. Hall
Alcoa Center, PA 15069

A. T. & T. Bell Laboratories
Attn: W. Brinkman
Murray Hill, NJ 07974

A. T. & T. Bell Laboratories
Attn: D. R. Hamann
Murray Hill, NJ 07974

A. T. & T. Bell Laboratories
Attn: Y. C. Chabal
Murray Hill, NJ 07974

A. T. & T. Bell Laboratories
Attn: M. J. Cardillo
Murray Hill, NJ 07974

A. T. & T. Bell Laboratories
Attn: J. C. Tully
Murray Hill, NJ 07974

Ames Laboratory
Iowa State University
221 Metals Development
Attn: J. H. Rose
Ames, IA 50011

Argonne National Laboratory
9700 S. Cass Avenue
Attn: D. M. Gruen
Argonne, IL 60439

Argonne National Laboratory
Materials Science Division, Bldg. 212
Attn: Dr. Dieter Wolf
9700 S. Cass Avenue
Argonne, IL 60439

Battelle Pacific Northwest
Attn: R. H. Jones
P. O. Box 999
Richland, WA 99352

Brookhaven National Laboratory
Attn: J. W. Davenport
Upton, Long Island, NY 11973

Brookhaven National Laboratory
Attn: K. Lynn
Upton, Long Island, NY 11973

Brookhaven National Laboratory
Attn: D. Welch
Upton, Long Island, NY 11973

Brown University
Department of Physics
Attn: P. J. Estrup
Providence, RI 02912

Dr. R. Bullough
Materials Development Div.
B552 Harwell Laboratory
Oxfordshire OX11 0RA
England

California Institute of Technology
Attn: T. C. McGill
Pasadena, CA 91125

California Institute of Technology
Attn: T. Tombrello
Pasadena, CA 91125

California Institute of Technology
Attn: W. H. Weinberg
Pasadena, CA 91125

Carnegie-Mellon University
Attn: A. W. Thompson
Dept of Met. Engr. and
Matls. Science
3325 Science Hall
Pittsburgh, PA 15213

Carnegie-Mellon University
Attn: P. Wynblatt
Dept of Met. Engr. and
Matls. Science
3325 Science Hall
Pittsburgh, PA 15213

Chemical Dynamics Corporation
Attn: M. J. Redmon, President
9560 Pennsylvania Avenue
Upper Marlboro, MD 20772

Cornell University
Bard Hall
Attn: H. Johnson
Ithaca, NY 14850

Cornell University
Bard Hall
Attn: J. M. Blakely
Ithaca, NY 14850

Cornell University
Laboratory of Atomic and Solid
State Physics
Attn: N. W. Ashcroft
Ithaca, NY 14853-2508

Eastman Kodak Company
Research Laboratories, Bldg. 81
Attn: Dr. J. R. Lavine
Rochester, NY 14650-2008

EG&G Idaho, Inc.
Attn: Clinton Van Siclen
Physics Group, MS 2211
P. O. Box 1625
Idaho Falls, ID 83415

Eindhoven University
Attn: H. H. Brongersma
Dept. of Physics
P. O. Box 513
5600 M. B. Eindhoven
The Netherlands

Fritz-Haber Institut
Faradayweg 4-6
Attn: G. Ertl
1000 Berlin 33
Federal Republic of Germany

Fysik Institut
Odense Universitat
Attn: P. Sigmund
DK-5230 Odense M
Denmark

Georgia Institute of Technology
Attn: Prof. Uzi Landman
225 North Avenue N.W.
Atlanta, GA 30332

Hahn-Meitner-Institut
Attn: H. Wollenberger
Glienicker Str. 100
1000 Berlin 39, West Germany

Harvard University
Attn: Prof. H. Ehrenreich
Cambridge, MA 02183

Harvard University
Attn: Prof. J. R. Rice
Cambridge, MA 02183

Harvard University
Attn: D. Vanderbilt
Cambridge, MA 02183

Haverford College
Department of Physics
Attn: L. Roelofs
Haverford, PA 19041

IBM Almaden Research
K33.801
Attn: Farid F. Abraham
650 Harry Road
San Jose, CA 95120-6099

I.B.M. Research Center
Attn: P. M. Marcus
P. O. Box 218
Yorktown Heights, NY 10598

I.B.M. Research Center
Attn: A. R. Williams
P. O. Box 218
Yorktown Heights, NY 10598

Imperial College
Dept. of Mathematics
Attn: Prof. D. G. Pettifor
London, SW7 2BZ
United Kingdom

Institut für Kristallographie
Universität München
Attn: R. J. Behm
Theresienstr. 41
D-8000, München
Federal Republic of Germany

Institut für Festkörperforschung der
Kernforschungsanlage
Attn: P. H. Dederichs
Postfach 1913
D-5170 Julich 1, West Germany

Institut für Festkörperforschung der
Kernforschungsanlage
Attn: H. Ibach
Postfach 1913
D-5170 Julich 1, West Germany

Institut für Festkörperforschung der
Kernforschungsanlage
Attn: W. Schilling
Postfach 1913
D-5170 Julich 1, West Germany

Institut für Festkörperforschung der
Kernforschungsanlage
Attn: H. Wenzl
Postfach 1913
D-5170 Julich 1, West Germany

Institut für Physikalische Chemie
Freie Universität Berlin
Attn: K. Christman
Takush. 3
1000 Berlin 33
Federal Republic of Germany

Interfaculty Reactor Institute
Attn: Dr. A. van Veen
Mekelweg 15
NL-2629JB, Delft
The Netherlands

International School for
Advanced Studies
Attn: V. Bortolani
I-34014 Trieste
Italy

International School for
Advanced Studies
Attn: Prof. F. Ercolessi
I-34014 Trieste
Italy

International School for
Advanced Studies
Attn: E. Tosatti
I-34014 Trieste
Italy

IRI
Delft University of Technology
Attn: A. van Veen
Mekelweg 15, N1-2629JB
Delft, The Netherlands

Iowa State University
Ames Laboratory
Attn: P. A. Thiel
Ames, IA 50011

Iowa State University
Ames Laboratory
Attn: A. E. DePristo
Ames, IA 50011

Iowa State University
Ames Laboratory
Attn: K.-M. Ho
Ames, IA 50011

Johns Hopkins University
Materials Science Department
Attn: K. Sieradzki
Baltimore, MD

Lab. Voor Fysische Metaalkunde
Materials Science Centre
Attn: J. Th. M. De Hosson
Groningen, Nijenborgh 18
The Netherlands

Lawrence Berkeley Laboratory
Materials and Molecular Res. Div.
Attn: M. L. Cohen
Berkeley, CA 94720

Lawrence Berkeley Laboratory
Materials and Molecular Res.Div.
Attn: S. G. Louie
Berkeley, CA 94720

Lawrence Berkeley Laboratory
Materials and Molecular Res. Div.
Attn: L. M. Falicov
Berkeley, CA 94720

Lawrence Berkeley Laboratory
Materials and Molecular Res.Div.
Attn: G. A. Somorjai
Berkeley, CA 94720

Lawrence Berkeley Laboratory
Materials and Molecular Res. Div.
Attn: M. A. van Hove
Berkeley, CA 94720

Los Alamos Natl. Scientific Lab.
P. O. Box 1663
Attn: D. L. Smith
Los Alamos, NM 87545

Los Alamos Natl. Scientific Lab.
P. O. Box 1663
Attn: A. Voter
Los Alamos, NM 87545

Los Alamos Natl. Scientific Lab.
P. O. Box 1663
Attn: S. P. Chen
Los Alamos, NM 87545

Loyola College
Deparment of Physics
Attn: Prof. R. S. Jones
4501 N. Charles St.
Baltimore, MD 21210

Massachusetts Institute of Technology
Attn: Prof. A. S. Argon
Cambridge, MA 02139

Massachusetts Institute of Technology
Dept. of Mat. Sci. & Eng.
Attn: Paul D. Bristowe
Cambridge, MA 02139

Massachusetts Institute of Technology
Attn: Prof. R. M. Latanision
Cambridge, MA 02139

Massachusetts Institute of Technology
Attn: S. Yip
Cambridge, MA 02139

Max-Planck-Institut für Plasmaphysik
Attn: R. Behrisch
D8046 Garching, West Germany

Max-Planck-Institut für Plasmaphysik
Attn: Professor V. Dose
D-8046 Garching, West Germany

Max-Planck-Institut für Metallforschung
Institut für Werkstoffwissenschaften
Attn: Dr. S. Schmauder
Seestrasse 92
7000 Stuttgart 1
Federal Republic of Germany

Max-Planck-Institut für Metallforschung
Institut für Werkstoffwissenschaften
Attn: Prof. Dr. Phil. H. Fischmeister
Seestrasse 92
7000 Stuttgart 1
Federal Republic of Germany

Max-Planck-Institut für Metallforschung
Institut für Werkstoffwissenschaften
Attn: Dr. W. Mader
Seestrasse 92
7000 Stuttgart 1
Federal Republic of Germany

Max-Planck-Institut für
Strömungsforschung
Attn: Prof. J. P. Toennies
Bunsenstrasse 10
D-3400 Göttingen
Federal Republic of Germany

Michigan Technological University
Materials Science Department
Attn: J. R. Waber
Houghton, MI 49931

National Institute of Standards
and Technology
Attn: J. M. Rowe, 235/A106
Washington, DC 20234

National Institute of Standards
and Technology
Materials Bldg., Rm. A 113
Attn: R. Thomson
Washington, DC 20234

Naval Research Laboratory
Attn: James Eridon, Code 4760
Washington, DC 20375

North Carolina State University
Attn: J. R. Beeler
Raleigh, NC 27607

Northwestern University
Dept. of Mat. Science & Engr.
Attn: Dr. David Seidman
2145 Sheridan Road
Evanston, IL 60201-9990

Oak Ridge National Laboratory
Bldg. 4500S, MS 6114
Box 2008
Attn: W. H. Butler
Oak Ridge, TN 37831-6114

Oak Ridge National Laboratory
P. O. Box X
Attn: H. L. Davis
Oak Ridge, TN 37830

Oak Ridge National Laboratory
P. O. Box X
Attn: J. Noonan
Oak Ridge, TN 37830

Oak Ridge National Laboratory
P. O. Box X
Attn: J. O. Steigler
Oak Ridge, TN 37830

Oak Ridge National Laboratory
P. O. Box X
Attn: M. Stocks
Oak Ridge, TN 37830

Oak Ridge National Laboratory
P. O. Box X
Attn: M. H. Yoo
Oak Ridge, TN 37830

Cornell University
Dept. of Matrerials Science
and Engineering
Attn: Prof. S. L. Sass
Ithaca, NY 14853-1501

The Ohio State University
Division of Materials Research
Attn: S. A. Dregia
Columbus, OH 43210

The Ohio State University
Attn: Prof. P. Shewmon
Dept. Matl. Sci. & Engr.
116 W. 19th Ave.
Columbus, OH 43210

The Ohio State University
Physics Department
Attn: J. W. Wilkins
174 West 18th Avenue
Columbus, OH 43210-1106

Pennsylvania State University
Attn: Barbara J. Garrison
Department of Chemistry
State College, PA 16801

Queens University
Dept. of Physics
Attn: Prof. Malcolm Stott
Stirling Hall
Kingston, Canada K7L 3N6

Rice University
Attn: Prof. R. B. McLellan
Houston, TX 77251

Rutgers University
Dept. of Ceramics
Attn: Dr. S. H. Garofalini
P. O. Box 909
Piscataway, NJ 08854

Paul Scherrer Institute
Attn: Dr. Alfredo Caro
5303 Wüerenlingen
Switzerland

Stanford University
Department of Chemistry
Attn: Prof. R. Zare
Stanford, CA 94305

Stanford University
Department of Chemical Engineering
Attn: Prof. R. Madix
Stanford, CA 94305

Technical University of Denmark
Attn: J. K. Nørskov
Lab. f. Technical Physics
DK-2800 Lyngby, Denmark

Texas A&M University
Dept. of Nuclear Engineering
Attn: Dr. R. Vijay
College Station, TX 77843

University of Aarhus
Institute of Physics
Attn: F. Besenbacher
DK-8000 Aarhus C, Denmark

University of Aarhus
Institute of Physics
Attn: J. Bottiger
Ivan Stensgaard
DK-8000 Aarhus C, Denmark

University of California
MANE Department
Attn: N. M. Ghoniem
6275 Boelter Hall
Los Angeles, CA 90024

University of California, Irvine
Department of Physics
Attn: Prof. A. Maradudin
Irvine, CA 92717

University of California, Irvine
Department of Physics
Attn: Prof. M. Mills
Irvine, CA 92717

University of Copenhagen
H. C. Ørsted Institute
Attn: H. H. Andersen
Universitetsperken 5
DK-2100 Copenhagen, Denmark

University of Illinois
Dept. of Mining and Metallurgy
Attn: H. K. Birnbaum
Urbana, IL 61801

University of Illinois
Nuclear Eng. Lab.
Attn: D. Ruzic
103 S. Goodwin Ave., Rm. 214
Urbana, IL 61801

University of Jyväskylä
Department of Physics
Attn: Prof. R. M. Nieminen
Seminaarinkatu 15
SF - 40100 Jyväskylä
Finland

The University of Liverpool
Dept. of Materials Science
and Engineering
Attn: Prof. D. J. Bacon
P. O. Box 147
Liverpool L69 3BX
England

University of Maryland
Department of Physics
Attn: T. Einstein
College Park, MD 20742-4111

University of Maryland
Department of Physics
and Astronomy
Attn: Dr. K. E. Khor
College Park, MD 20742-4111

Michigan Technological University
Dept. of Metallurgical Engineering
Attn: J. K. Lee
Houghton, MI 49931

University of Michigan
Dept. of Mat. Sci. and Engr.
Attn: D. Srolovitz
Ann Arbor, MI 48109-2136

University of Michigan
Department of Nuclear Engineering
Attn: G. Was
Ann Arbor, MI 48109

University of Minnesota
Dept. of Chemical Engr. and
Materials Science
Attn: J. R. Chelikowsky
151 Amundson Hall
421 Washington Avenue S. E.
Minneapolis, MN 55455

University of Minnesota
Corrosion Research Center
Attn: R. A. Oriani
Minneapolis, MN 55455

University of Minnesota
Corrosion Research Center
Attn: W. W. Gerberich
Minneapolis, MN 55455

University of New Mexico
Chemistry & Nuclear Eng. Dept.
Attn: Dr. Anil Prinja
Albuquerque, NM 87131

University of Pennsylvania
Department of Materials Science
Attn: V. Vitek
Philadelphia, PA 19104

University of Notre Dame
Dept. Physics
Attn: J. Dow
Box E
Notre Dame, IN 46556

University of Pennsylvania
LRSM Building, Room 400
Attn: Thomas M. Buck
3231 Walnut Street
Philadelphia, PA 19104-6272

University of Texas
Departments of Astronomy and Physics
RLM 15-212
Attn: R. Smoluchowski
Austin, TX 78712

University of Trieste
Dipartimento di Fisica Teorica
Attn: Prof. N. Parrinello
I-34014 Trieste
Italy

University of Virginia
Department of Materials Science
Attn: R. A. Johnson
School of Engineering and
Applied Science
Charlottesville, VA 22901

University of Wisconsin
ECE Department
Attn: Prof. W. N. G. Hitchon
Madison, WI 53706

Utica College
Physics Department
Attn: Dr. Majid Karimi
Utica, NY 13502

Virginia Commonwealth University
Dept. of Physics
Attn: Prof. P. Jena
Richmond, VA 23284-2000

Virginia Commonwealth University
Dept. of Physics
Attn: Prof. T. McMullen
Richmond, VA 23284-2000

West Virginia University
Dept. of Physics
Attn: Bernard R. Cooper
Morgantown, WV 26506

Washington University
Department of Physics
Campus Box 1105
Attn: Anders Carlsson
St. Louis, MO 63130

Washington State University
Dept. of Mechanical and
Materials Engineering
Attn: Richard Hoagland
Pullman, WA 99164-2920

Xerox PARC
Attn: D. J. Chadi
3333 Coyote Hill Road
Palo Alto, CA 94304

R. M. Alire, L-358
T. D. de la Rubia, L-644
M. W. Guinan, L-396
W. E. King, L-386
E. C. Sowa, L-356
M. J. Weber, L-365

1000 V. Narayanamurti
1090 J. E. Schirber
1100 F. L. Vook
1110 S. T. Picraux
1111 B. L. Doyle
1112 S. M. Myers
1112 W. R. Wampler
1134 G. L. Kellogg
1143 B. W. Dodson
1145 G. C. Osbourn
1151 D. Emin
1151 D. R. Jennison
1823 J. A. Borders
1830 M. J. Davis
2500 R. L. Schwoebel
5100 H. W. Schmitt
6000 D. L. Hartley
7121 W. G. Perkins
7400 J. C. King

8000 J. C. Crawford
Attn: 8100 E. E. Ives
8200 R. J. Detry
8400 R. C. Wayne
8500 P. E. Brewer
8230 W. D. Wilson
8233 J. Harris
8233 R. Cline
8233 C. L. Bisson
8240 C. W. Robinson

8300 P. L. Mattern
Attn: 8310 R. W. Rohde
8350 J. S. Binkley
8360 W. J. McLean
8314 J. E. Costa
8314 M. W. Perra
8314 N. R. Moody
8314 S. Robinson
8340 W. Bauer
8341 M. I. Baskes
8341 J. B. Adams
8341 M. S. Daw
8341 S. M. Foiles
8341 R. B. James
8341 D. D. Johnson (10)
8341 J. S. Nelson
8341 R. B. Phillips
8341 C. M. Rohlfing
8341 G. J. Thomas
8341 W. G. Wolfer
8341 Files
8342 M. Lapp
8343 R. H. Stulen
8343 T. E. Felter
8343 S. E. Guthrie
8343 G. D. Kubiak
8347 K. L. Wilson
8357 C. F. Melius

8535 Publication Div./ Technical Library Processes Div., 3141

3141 Technical Library Processes Div. (3)

8524-2 Central Technical Files (3)

Org.	Bldg.	Name	Rec'd by	Org.	Bldg.	Name	Rec'd by

Sandia National Laboratories